Chapter 2

Carbon nanotubes network ambipolar field effect transistors with 10^8 on/off ratio

In this chapter we introduce blade coating technique for fabrication of FETs with semi-aligned polymer wrapped SWNTs in the channel. We demonstrate highly performing ambipolar FETs with carrier mobilities ranging from 0.42 $cm^2/V{\cdot}s$ to 3.71 $cm^2/V{\cdot}s$ and recordly high on/off ratio of 10^8. Semiconducting SWNTs were selected by polymer wrapping method using poly-9,9-di-n-dodecyl-fluorenyl-2,7-diyl (PF12) and poly(3-dodecylthiophene-2,5-diyl) (P3DDT). Furthermore, we found out that the wrapping polymer has influence not only on the quality of SWNTs dispersion, but also on the device performance. The FETs based on PF12-wrapped SWNT shows almost symmetric ambipolar characteristic, while the devices fabricated with P3DDT-wrapped SWNTs demonstrate significantly lower electron current. Additionally, we discuss importance of the control of wrapping polymer concentration as it has significant influence on transport characteristics of FETs.

V. Derenskyi, W. Gomulya, J. M. Salazar Rios, M. Fritsch, N. Fröhlich, S. Jung, S. Allard, S. Z. Bisri, P. Gordiichuk, A. Herrmann, U. Scherf, and M. A. Loi, *Adv. Mater*. **2014**, *26*, 5969-5975

2.1 Introduction

Owing to their unique one-dimensional **s**tructure, single walled carbon nanotubes (SWNTs) possess outstanding near-ballistic transport properties which make them one of the leading candidates to replace silicon in the fabrication of high-speed and low-voltage field-effect transistors (FET). In fact, SWNTs, unlike graphene, have a substantial bandgap and display semiconducting properties. SWNTs can be classified as intrinsic semiconductors, which allow full control of the state (on or off) of the FETs by applying a gate voltage. Interestingly, these transistors are equally able to accumulate electrons and holes, thus allowing the fabrication of FETs that can change polarity depending on the applied gate voltage (ambipolar).

Complementary metal-oxide-semiconductor (CMOS) devices are fundamental components of integrated circuits. In the standard configuration n- and p-type FETs are used to obtain different functions. CMOS-like devices fabricated using two ambipolar FETs would allow the reduction of the number of fabrication steps, thus reducing the effort necessary for the fabrication of logic circuits.[1] Besides the need for CMOS-like devices, a high on/off ratio is required by many different FET applications, including driving electronics for displays (on/off $>10^7$) and resistance-based memories ($>10^8$).[2]

However, achieving the required high on/off ratio and mobility necessary for these applications with SWNTs FET is still a great challenge. In principle, state-of-the-art single-strand SWNT FETs can meet these requirements of high mobility and high on/off ratio.[3,4] However, their fabrication procedure is not suitable for large scale production, and does not show the high reproducibility required for high throughput device fabrication.[4] An alternative strategy is to use solution-processed SWNTs networks, which so far have not demonstrated their full potential due to the random distribution of nanotubes of different species in the transistor channel.

The alignment of SWNTs in the transistor channel can significantly improve the device performance.[5] Several efforts to align SWNTs have been made utilizing techniques such as Langmuir-Schaefer deposition,[6] chemical self-assembly,[7] and dielectrophoresis (DEP).[8] In general, aligned SWNT networks demonstrated higher charge carrier mobility than random networks. However, the state-of-the-art on/off ratio for FETs made using these

methods still remains low (10^5), which hampers practical applications. One of the causes is the low purity of the semiconducting SWNT solutions. Exposure to oxygen and water also has a detrimental effect on the off current and transforms the transistors into p-type.[9]

Among the many techniques[10-12] developed in the past several years to select semiconducting single-walled carbon nanotubes (sSWNT) from a mixture, one of the most interesting is the polymer-assisted separation method, because of its high effectiveness and scalability.[13] Recently, we reported highly enriched selection of small diameter semiconducting nanotubes using polyfluorene derivative (PF8).[14-16] Later, we demonstrated that nanotubes with various diameters, including large diameter ones (ca. 1.5 nm), can be selected by exploiting polyfluorene derivatives bearing side chains of different lengths.[17] Nevertheless, polyfluorenes are not the only conjugated polymers able to select sSWNTs. Recently, it was demonstrated that poly(3-dodecylthiophene-2,5-diyl) is very efficient in sorting semiconducting carbon nanotubes.[18]

2.2 Semi-aligned SWNTs network by blade coating

Here we report the fabrication of high-performance FETs showing a record on/off ratio of 10^8 in simple device geometry with bottom contact and bottom gate with channel length of 10 µm. The devices were obtained with semi-aligned polymer wrapped SWNT networks deposited on SiO_2 dielectric by blade coating from solutions using different types of polymers, namely, poly-9,9-di-n-dodecyl-fluorenyl-2,7-diyl (PF12) and poly(3-dodecylthiophene-2,5-diyl) (P3DDT). The blade coating technique (**Figure 1**a) allows the alignment of SWNTs in the transistor channel and achieves an enhancement of the device parameters to record values. Interestingly, several device parameters appear to be influenced by the nature of the polymer used for the selection of the semiconducting tubes. We rationalize this effect in terms of the relative position of the energy levels of the polymer and the SWNTs.

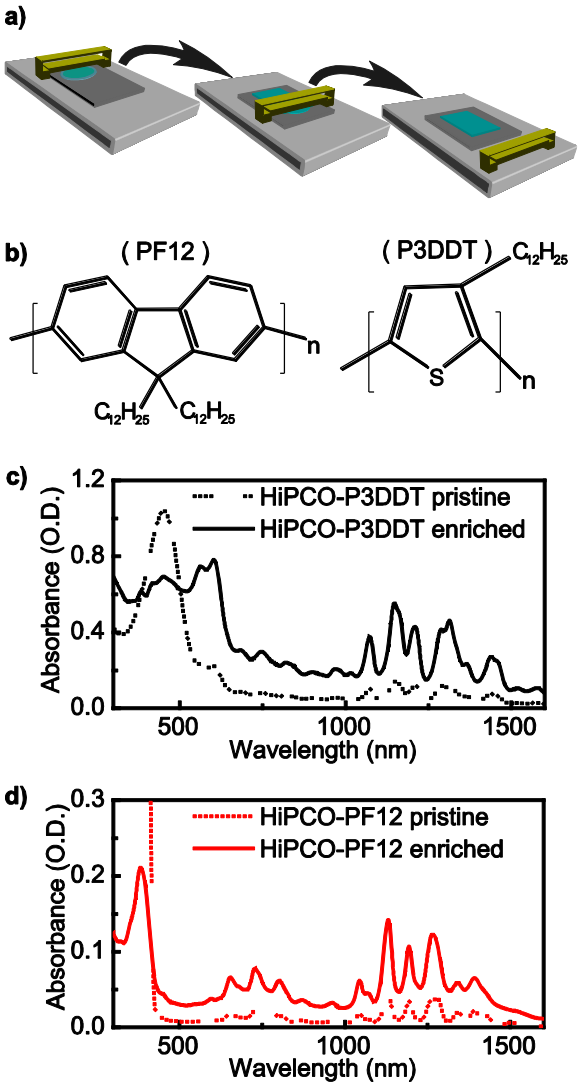

Figure 1. (a) Schematic illustration showing the process of blade coating. (b) Chemical structures of poly-9,9-di-n-dodecyl-fluorenyl-2,7-diyl (PF12) and Poly(3-dodecylthiophene-2,5-diyl). (c) Absorption spectra of the pristine (dashed line) and enriched (solid line) P3DDT-wrapped HiPCO SWNT solution. (d) Absorption spectra of the pristine (dashed line) and enriched (solid line) PF12-wrapped HiPCO SWNT solution.

To select the semiconducting species from the starting mixture of nanotubes produced by high-pressure carbon monoxide conversion (HiPCO), we utilized two different polymer backbones, PF12 and P3DDT (Figure 1b**)**, which both have alkyl side chains with 12 carbon atoms. The preparation of the solution comprises two major steps, sonication and ultracentrifugation.[14,17] Through sonication, we are able to de-bundle and disperse nanotubes in the organic solvent polymer solution. By ultracentrifugation, contaminants, bundles and undispersed metallic species are removed. In this way, a rather diluted dispersion of sSWNTs (ca. 6.5 µg/ml for PF12-wrapped and ca. 54 µg/ml for P3DDT-wrapped) containing a large amount of excess polymer was obtained. Therefore, to obtain a higher concentration of SWNTs and to reduce the amount of excess polymer, a further enrichment step was necessary. The enrichment, as we have reported previously, requires a precipitation of the sSWNTs initially selected as the supernatant, a washing step to eliminate the excess polymer, and a re-dispersion.[17]

The absorption spectra of PF12-wrapped HiPCO (PF12-SWNT) and P3DDT-wrapped HiPCO (P3DDT-SWNT) solutions before and after the enrichment are shown in Figures 1c and d, respectively. We can clearly observe the reduction of the polymer peaks below 400 nm (PF12) and 600 nm (P3DDT) in the spectra of the enriched solution obtained with both polymers. At the same time, the intensity of the peaks corresponding to sSWNT increases in the range between 1000 nm and 1500 nm. From the absorption of the solution and using cross sections for absorption reported in the literature,[19] we estimated the enrichment process to give rise to concentrations of sSWNTs of approximately 23 µg/ml for PF12-SWNTs and ca. 210 µg/ml for dispersions made with P3DDT.

The ink obtained in this way can be used with every solution processing technique. In this chapter we compare the blade coating method (Figure 1a) with simple drop-casting technique, which we have previously exploited successfully for device fabrication.[14]

Blade coating is a very attractive technique for large volume and large area device fabrication, being highly scalable and reproducible. In terms of technical challenges, deposition by blade coating of the sSWNTs ink is far easier and faster than DEP and Langmuir-Schaefer assembly. Moreover, in blade coating, SWNTs are aligned during the deposition process.

2.3 PF12 and P3DDT-wrapped SWNTs for FETs fabrication

Two batches of SWNT FETs were fabricated from PF12-SWNT and P3DDT-SWNT enriched solutions by using both drop-casting and blade coating. The drop-casting samples were fabricated following the same procedure as previously reported for small diameter nanotubes wrapped with PF8.[14]

Figure 2a shows an atomic force microscopy (AFM) image of carbon nanotubes (CNTs) randomly distributed in the channel for drop-cast films, while Figure 2b shows the SWNT network deposited by blade coating. Blade coating results in a partial alignment of the nanotubes along the direction of the blade movement. An alignment ratio of up to 52% is obtained by this method. This value is the result of counting the number of tubes aligned within ± 30° of the preferred orientation in the AFM pictures of the transistor channel. Because of the high aspect ratio of the nanotubes, we expect there to be a larger number of connections between the source-drain electrodes and the nanotubes in this semi-aligned sample, thus increasing the maximum current of the transistor in the on-state and leading to higher charge carrier mobility.

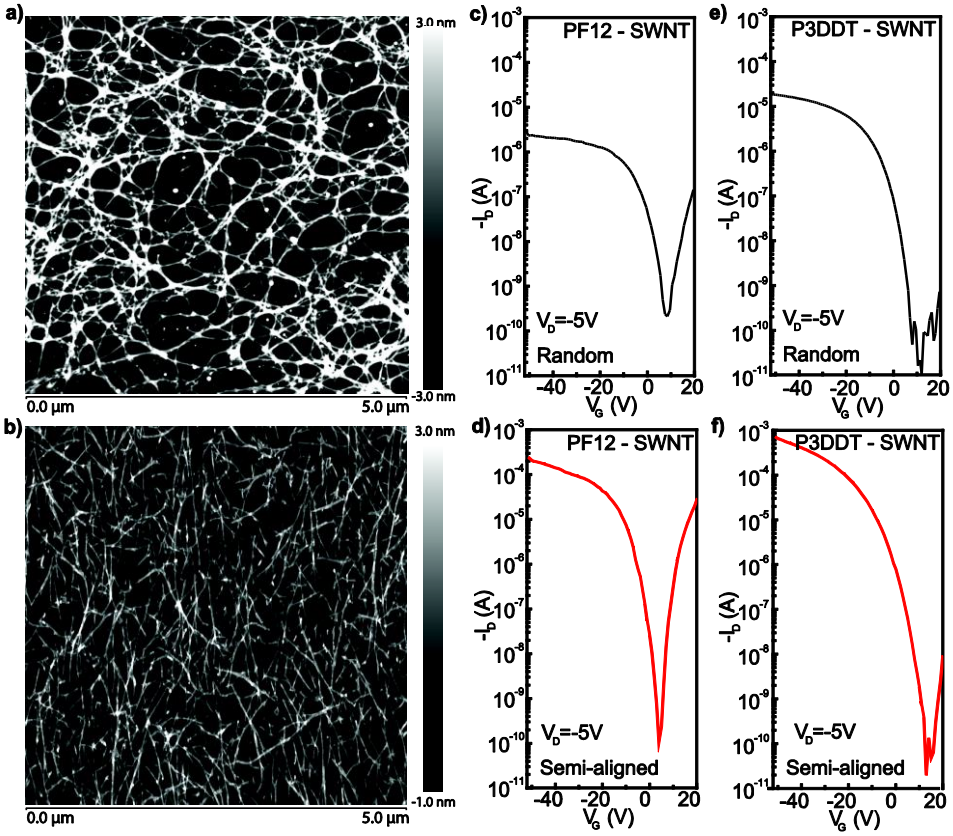

Figure 2. AFM image in tapping mode of the FET channel area showing (a) Random SWNT network deposited by drop-casting and (b) Semi-aligned SWNT network deposited by Blade coating. The heights in the image are indicated with the color barcodes on the right. ID-VG transfer characteristics of FETs measured at V_D = -5 V corresponding to (c) Random PF12-SWNT network; (d) Semi-aligned PF12-SWNT network; (e) Random P3DDT-SWNT network; (f) Semi-aligned P3DDT-SWNT network.

I_D-V_G transfer characteristics of the random and semi-aligned PF12-SWNT network FETs are reported in Figure 2c and d, respectively. The random-network FET fabricated with PF12-SWNT shows an on/off ratio of only 10^4 for the hole current. The sample deposited by blade coating displays an on/off ratio as high as 3×10^6 at V_D = -5 V (Figure 2d). The on-current in the semi-aligned network increases from 30 µA to 0.2 mA

and the hole mobility improves from 9.00×10^{-3} $cm^2/V \cdot s$ to 2.17 $cm^2/V \cdot s$. Such a drastic improvement in the on/off ratio and carrier mobility arises from the reduction of the number of nanotube-nanotube intersections in the transistor channel on going from the random to the aligned network. Cross junctions are known to be one of the main causes of carrier trapping and mobility losses, especially because the polymer wrapped around the nanotubes can act as an additional barrier (or trap) to charge transport through the network.

Figure 2e and f show a comparison between the transfer characteristics in the linear regime of P3DDT-SWNT FETs fabricated by drop casting and blade coating, respectively. The devices fabricated with P3DDT-SWNT are strongly dominated by hole transport. Moreover, the transfer characteristics of both the drop-cast and semi-aligned FETs display a considerable shift (20 V) of the threshold towards positive gate voltages. Similarly to what was obtained with PF12-SWNT FETs, the aligned P3DDT-SWNT nanotube devices demonstrated higher on/off ratio, up to 7×10^7, compared with 4×10^5 in the random network device. The FETs fabricated with semi-aligned P3DDT-SWNTs also exhibited higher mobility (3.71 $cm^2/V \cdot s$) than the random network (0.03 $cm^2/V \cdot s$). It is important to underline that the hole on/off ratio of 7×10^7 is the highest ever reported for any solution-processed SWNT network FETs and for any solution processed semiconductor, especially on SiO_2 dielectric.

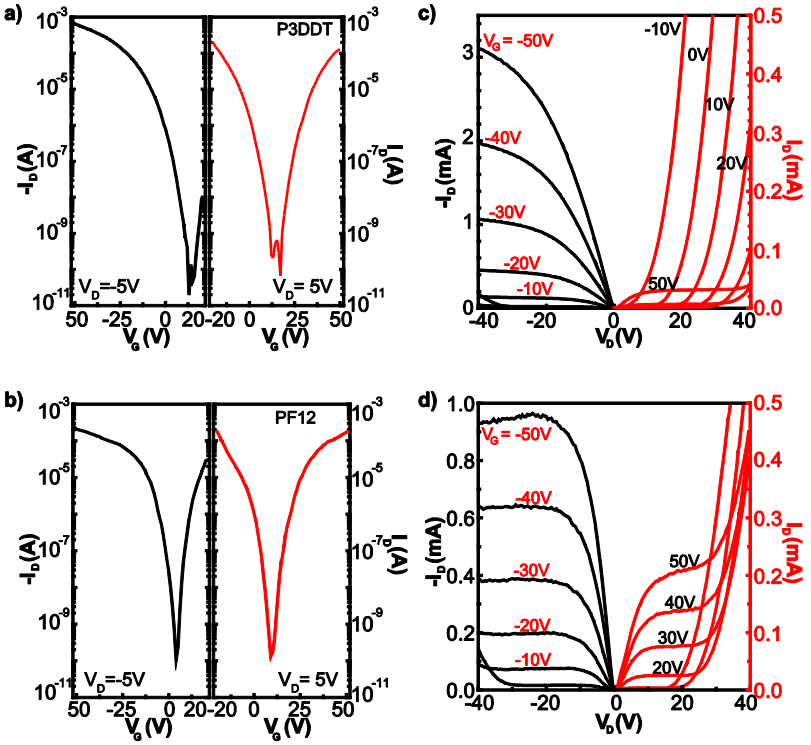

Figure 3. I_D-V_G transfer and I_D-V_D output characteristics of FETs fabricated with P3DDT-wrapped- sSWNT (a and c) and with PF12-wrapped- sSWNT (b and d).

Figure 3 depicts the full characterization of the FETs fabricated with the P3DDT- and PF12-wrapped SWNT aligned network (The transfer characteristics measured in saturation regime (±25 V) and the gate current of all devices are demonstrated on **Figure 4**). From the output characteristics shown in Figure 3c,d it is evident that the devices fabricated with P3DDT wrapped SWNTs have a much lower electron contribution than the devices fabricated with PF12-wrapped SWNT. An estimate of the electron current difference between the two samples can be obtained from the transfer characteristics measured at V_D= +5 V (Figure 3a,b). About one order of magnitude difference in current can be seen between P3DDT-SWNTs and PF12-SWNTs. For a given gate voltage, the PF12–based FET shows quite symmetric electron and hole contributions, while in the case of P3DDT we observe predominantly p-type characteristics.

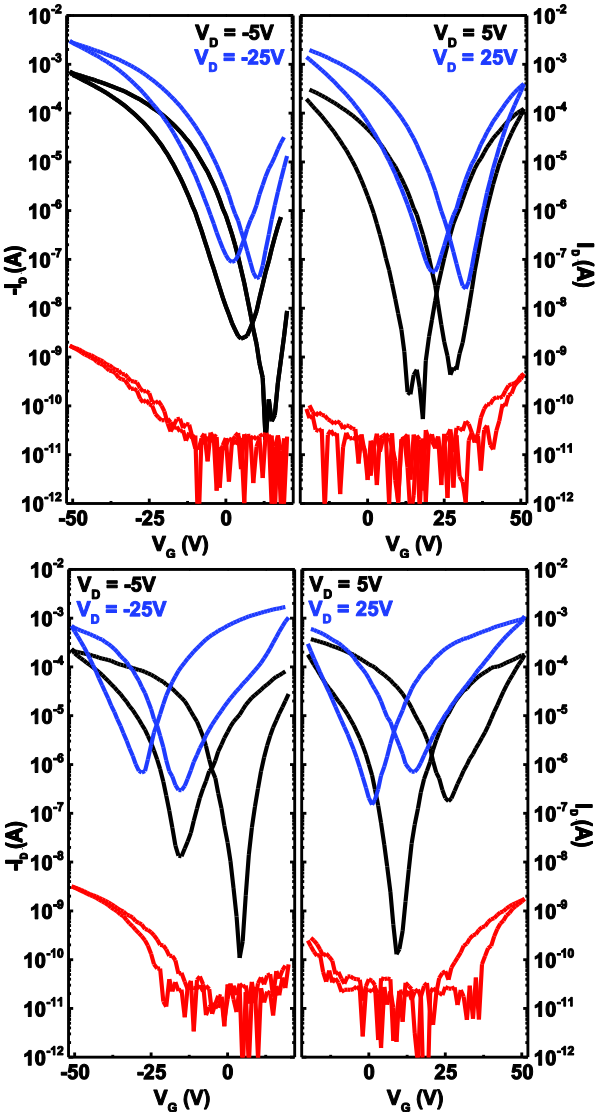

Figure 4. I_G-V_G characteristics (red line) and I_D-V_G characteristics showing hysteresis (black line) of FETs fabricated with P3DDT-wrapped-sSWNT (Fig.3a) and PF12-wrapped sSWNT (Fig.3b). V_G was swept from -50 V to 50 V.

As mentioned previously, the threshold voltage of the devices fabricated with PF12-SWNTs and P3DDT-SWNTs show a difference of about 10V. Since the solution preparation and device fabrication were identical for both polymer-wrapped SWNT samples, we can attribute the differences observed in the device characteristics to the nature of the nanotube-polymer interaction or to the properties of the polymers themselves.

2.4 The origin of the charge transport difference

To understand the origin of the different ratios between the electron and hole currents and of the difference in the threshold voltage shift, we compare the transport characteristics of FETs fabricated from SWNTs enriched solutions and those fabricated from pristine (without enrichment) solutions produced with both polymers. The dashed and solid lines in **Figure 5**a show the I_D-V_G transfer characteristics of FETs prepared using pristine and enriched PF12-SWNT solutions, respectively. Both devices exhibit ambipolar behavior with maximum hole mobility of 2.17 $cm^2/V{\cdot}s$ and maximum electron mobility of 0.86 $cm^2/V{\cdot}s$ measured for enriched solutions. The on/off ratio for hole accumulation increases from 5×10^4, in FETs fabricated from pristine solutions, to 3×10^6 in devices made with the enriched solution. Figure 5b shows a detail of the device transfer characteristics from which the threshold voltage values are extracted. The threshold voltage for hole accumulation is found to be -17.5 V (dashed line) for the device fabricated with the pristine solution and -7.5 V (solid line) for the one fabricated with the enriched dispersion. This difference can be explained by the excess polymer in the pristine solution that might act as a barrier hindering the transport between tubes, but also might function as a trap, decreasing the number of carriers in the transistor channel. Consequently, the removal of the excess polymer in the enrichment process improves the hole accumulation and shifts the threshold by about 10V towards $V_G = 0$ V.

Figure 5c shows the I_D-V_G transfer characteristics of FETs fabricated from P3DDT-SWNT solution with and without enrichment treatment. The highest hole mobility values are 0.42 $cm^2/V{\cdot}s$ for non-enriched and 3.71 $cm^2/V{\cdot}s$ for enriched solutions, respectively. Removing the excess of polymer in the case of P3DDT-SWNT gives rise to higher on/off ratio which reaches values of 7×10^7. The off current decreases from ca. 100 pA to ca. 10 pA in devices fabricated with enriched dispersion, while the on-current increases slightly, 0.5 mA (pristine) and 0.7 mA (enriched). In contrast to our findings for PF12-SWNT-based devices, we observe only very small threshold voltage difference

between devices fabricated with the pristine P3DDT-SWNT (-20.5 V) and enriched solutions (-18.5 V). Moreover, while the enrichment of PF12-SWNT solution resulted in an improvement of the device ambipolarity, this is not the case for P3DDT-SWNT.

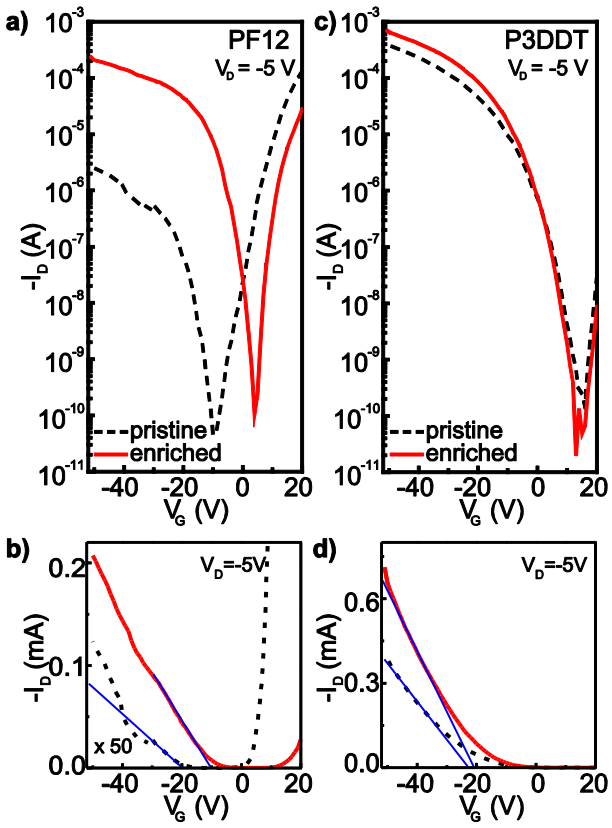

Figure 5. Comparison of I_D-V_G transfer characteristics of the FETs based on (a) Pristine and enriched PF12-wrapped-HiPCO sSWNT solution; (c) Pristine and enriched P3DDT-wrapped-HiPCO sSWNT solution. Comparison of the threshold voltages for pristine (dashed line) and enriched (solid line) solutions of sSWNTs wrapped by (b) PF12 polymer; and (d) P3DDT polymers.

Polymer chains wrapped around the carbon nanotubes could in principle have a beneficial role, in particular when using SiO_2 as the gate dielectric, screening charges from trapping sites in the dielectric. However, an excess of polymer between the SWNTs

suppresses the charge transport between the tubes because of the high energetic barrier between the nanotubes and the polymer.[14]

Both P3DDT and PF12 exhibit a bandgap wider than that of HiPCO sSWNTs. As a consequence, charge carrier transport can be hindered by the barrier between the energy levels of sSWNT and the polymer. In the case of polythiophene, the difference between the HOMO (highest occupied molecular orbital) and LUMO (lowest unoccupied molecular orbital) levels of the polymer and (6,5) sSWNT is approximately 0.3 eV and 0.5 eV, respectively. Polyfluorene has a wider bandgap, thus forming a higher energy barrier (about 1 eV) for electron and hole transport through the polymer. Further investigations are under way to validate the above model.

To place our results in the context of state-of-the-art of CNT-network electronics, we compared the performance of our devices with that reported by other researchers.[5,6,18,20-28] **Figure 6** summarizes all SWNT network FETs fabricated on SiO_2/Si gates worldwide. The devices based on PF12-SWNT solution with semi-aligned networks are superior with respect to the effective mobility and on/off ratio, for both electrons and holes, in relation to PF8-SWNT FETs that were previously reported by our group.[14] Certainly, PF12 wrapping provides HiPCO solution with much higher nanotube concentrations than PF8,[17] but also the alignment of the nanotubes significantly contributes to the high mobility and high on/off ratio. The achieved on/off ratio values are comparable with results obtained in single-strand SWNT ambipolar FET.[3]

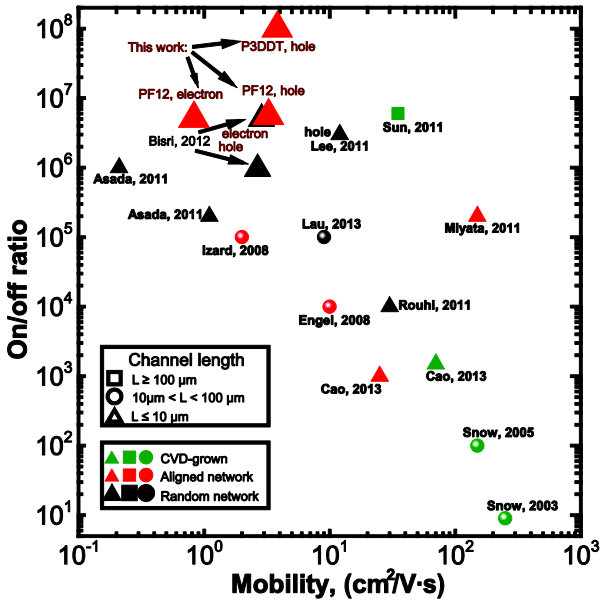

Figure 6. Performance map of SWNTs FET fabricated with CVD and solution-processes. The FETs with aligned and random SWNTs networks fabricated from solution are depicted with red and black symbols, respectively. The devices are categorized also according to their channel length.

The hole branch of P3DDT-SWNT FETs demonstrates a record average on/off ratio of 7×10^7 with channel lengths shorter than 10 µm. This value is the highest ever reported for both solution-processed and chemical vapor deposition (CVD)-grown SWNT.

The achievement of very high on/off ratio in these devices derives from various factors: i) the precise control of the polymer wrapping mechanism, which guarantee samples of high purity in terms of semiconducting species; ii) the high concentration of the semiconducting tubes in the starting solution and the reduction of the polymer content achieved with the enrichment procedure; iii) the alignment of the SWNTs through the blade coating technique.

2.5 Conclusion

In conclusion, we have reported the fabrication of FETs with semi-aligned polymer-wrapped carbon nanotube networks with effective carrier mobilities ranging from 0.42 $cm^2/V \cdot s$ to 3.71 $cm^2/V \cdot s$ and a record on/off ratio of 10^8. Interestingly, the wrapping polymer is found not only to influence the SWNT dispersion in terms of quantity of semiconducting tubes but also to tune the FET performance. While PF12-wrapped networks show almost symmetric ambipolar characteristics, samples fabricated with P3DDT-wrapped-SWNTs show much lower electron current. The polymer concentration reduction through the enrichment process is found to be an important factor in modifying the transport characteristics of the PF12-SWNT-FETs, especially by influencing the electron threshold voltage. The effectiveness and scalability of the nanotube network deposition and alignment as well as the ability to control ambipolarity by polymer wrapping are expected to broaden the range of SWNT-FET applications in both high-performance and large-area electronics. The high on/off ratio obtained for these devices is compatible with the highest demand applications for field effect transistors.

2.6 Experimental section

Preparation and characterization of the semiconducting SWNT dispersion: The P3DDT (M_n = 43800, M_W = 47500) and PF12 (M_n = 162000, M_W = 373000) polymers were solubilized in toluene, with concentration 3 mg per 10 ml of solvent. Subsequently, single-walled HiPCO (High Pressure Carbon Monoxide) carbon nanotubes (3 mg; Unidym, Sunnyvale, CA) were added. The solution was then sonicated with an ultrasonic liquid processor (Sonicator 3000, QSonica, Newtown, CT) for 2 hours at 69 W and 16°C. Two-step centrifugation was performed to remove bundles, carbon contaminants, and metallic nanotubes, as well as to enrich the SWNT solution. During the first ultracentrifugation with an Optima XE-90 instrument (Beckman Coulter, Brea, CA; rotor: SW55Ti) (1 h, 40 000 rpm, 190000 *g*), the high density components precipitated, forming a pellet at the bottom of the centrifugation tube, while the low density components, containing individualized sSWNTS wrapped with polymer, stayed in the upper part as the supernatant. The second step (5 h, 55000 rpm, 367000 *g*) was used in order to enrich SWNTs and to remove excess polymer.[14] Here, individualized sSWNTs are precipitated to form a pellet. Finally, the pellet was re-dispersed in 2 mL toluene. The purity of the nanotube solution was examined

by absorption spectroscopy using a UV/vis/NIR spectrophotometer (Shimadzu UV 3600). The spectra of the HiPCO nanotube solution were recorded in the range between 300 nm and 1600 nm. From the absorption measurements the concentration of the sSWNTs in different samples was estimated using the calculated cross section for absorption of carbon.[19]

Fabrication of SWNT transistors: Nanotubes were deposited on a highly doped silicon wafer with 230 nm thick SiO_2 dielectric. The source and drain electrodes were defined by a bilayer of ITO (10 nm) and Au (30 nm), forming a transistor channel of 10 µm length and 10 mm width. Two techniques, drop-casting[14] and blade coating, were used for nanotube deposition. The equipment (Zehntner ZAA 2300 automatic film applicator coater, Zehntner, Sissach, Switzerland) used for SWNT deposition is shown schematically on Figure 1a. The setup consists of a heating plate and an aluminum blade, which can move with variable speed above the plate. The distance between the blade and the substrate can be adjusted with two micrometer-sized screws. Silicon chips were placed on top of hot glass and heated up to 55°C. SWNT solution (20 µl) was dropped on the chip and the excess solution was removed by the flat blade moving above the substrate. The process of deposition was repeated 10 times to increase the density of nanotube network. The substrate was subsequently annealed in nitrogen atmosphere at 140°*C* for 3 h to remove the residual organic solvent.

Characterization of the SWNT transistor: Electrical measurements were performed using a probe station placed in a nitrogen-filled glovebox at room temperature under dark conditions. The probe station was connected to an Agilent E5270B Semiconductor Parameter Analyzer with resolution of 10 fA. All devices were measured without being exposed to air from the beginning of the SWNT deposition process until the electrical characterization. The effective mobility values were extracted from the linear regime of the I_D-V_G transfer characteristics at V_{DS} = ±5 V for both p- and n-channels. Since the density of the nanotube network (51/µm^2) in all devices was above the percolation limit (6/µm^2), the parallel plate model was used to calculate the capacitance of the gate dielectric. The quantum capacitance of the nanotube was not taken into account, so the total capacitance values were overestimated; thus the effective mobility values are underestimated. The threshold voltages were extracted using extrapolation of drain current intercept, which is a standard textbook method as describe by Sze and Ng.[29]

Characterization of SWNT networks by AFM: The SWNT networks within the channel of the FETs were imaged by AFM in tapping mode. The scanning region was the channel area, exhibiting a size of 20 μm^2. The images were recorded using a Bruker MultiMode 8 Microscope with TESP probes (spring constant k = 42 $N \cdot m^{-1}$, resonance frequency f in the range 320–410 kHz, and tip radius less than 10 nm). The scan rate and resolution of the measurements were selected to be 1 Hz and 1024 lines per sample, respectively. For each image a new probe was employed to avoid AFM tip broadening as a result of wear or contaminations from the conjugated polymer. The AFM images were analysed with Bruker NanoScope Analysis software.

2.7 References

[1] S. Z. Bisri, C. Piliego, J. Gao, and M. A. Loi, "Outlook and Emerging Semiconducting Materials for Ambipolar Transistors," *Adv. Mater.*, vol. 26, no. 8, pp. 1176–1199, 2014.

[2] "International Technology Roadmap for Semiconductors, Emerging Research Devices," vol. 2011.

[3] A. D. Franklin and Z. Chen, "Length scaling of carbon nanotube transistors," *Nat. Nanotechnol.*, vol. 5, no. 12, pp. 858–862, Dec. 2010.

[4] A. D. Franklin, M. Luisier, S. Han, G. Tulevski, C. M. Breslin, L. Gignac, M. S. Lundstrom, and W. Haensch, "Sub-10 nm Carbon Nanotube Transistor," *Nano Lett.*, vol. 12, no. 2, pp. 758–762, Feb. 2012.

[5] M. Engel, J. P. Small, M. Steiner, M. Freitag, A. A. Green, M. C. Hersam, and P. Avouris, "Thin Film Nanotube Transistors Based on Self-Assembled, Aligned, Semiconducting Carbon Nanotube Arrays," *ACS Nano*, vol. 2, no. 12, pp. 2445–2452, Dec. 2008.

[6] Q. Cao, S. Han, G. S. Tulevski, Y. Zhu, D. D. Lu, and W. Haensch, "Arrays of single-walled carbon nanotubes with full surface coverage for high-performance electronics," *Nat. Nanotechnol.*, vol. 8, no. 3, pp. 180–186, Mar. 2013.

[7] H. Park, A. Afzali, S.-J. Han, G. S. Tulevski, A. D. Franklin, J. Tersoff, J. B. Hannon, and W. Haensch, "High-density integration of carbon nanotubes via chemical self-assembly," *Nat. Nanotechnol.*, vol. 7, no. 12, pp. 787–791, Dec. 2012.

[8] S. Shekhar, P. Stokes, and S. I. Khondaker, "Ultrahigh Density Alignment of Carbon Nanotube Arrays by Dielectrophoresis," *ACS Nano*, vol. 5, no. 3, pp. 1739–1746, Mar. 2011.

[9] V. Derycke, R. Martel, J. Appenzeller, and P. Avouris, “Controlling doping and carrier injection in carbon nanotube transistors,” *Appl. Phys. Lett.*, vol. 80, no. 15, pp. 2773–2775, Apr. 2002.

[10] N. Komatsu and F. Wang, “A Comprehensive Review on Separation Methods and Techniques for Single-Walled Carbon Nanotubes,” *Materials*, vol. 3, no. 7, pp. 3818–3844, Jun. 2010.

[11] M. C. Hersam, “Progress towards monodisperse single-walled carbon nanotubes,” *Nat. Nanotechnol.*, vol. 3, no. 7, pp. 387–394, Jul. 2008.

[12] W. Gomulya, J. Gao, and M. A. Loi, “Conjugated polymer-wrapped carbon nanotubes: physical properties and device applications,” *Eur. Phys. J. B*, vol. 86, no. 10, pp. 1–13, Oct. 2013.

[13] A. Nish, J.-Y. Hwang, J. Doig, and R. J. Nicholas, “Highly selective dispersion of single-walled carbon nanotubes using aromatic polymers,” *Nat. Nanotechnol.*, vol. 2, no. 10, pp. 640–646, Oct. 2007.

[14] S. Z. Bisri, J. Gao, V. Derenskyi, W. Gomulya, I. Iezhokin, P. Gordiichuk, A. Herrmann, and M. A. Loi, “High Performance Ambipolar Field-Effect Transistor of Random Network Carbon Nanotubes,” *Adv. Mater.*, vol. 24, no. 46, pp. 6147–6152, 2012.

[15] J. Gao, M. A. Loi, E. J. F. de Carvalho, and M. C. dos Santos, “Selective Wrapping and Supramolecular Structures of Polyfluorene–Carbon Nanotube Hybrids,” *ACS Nano*, vol. 5, no. 5, pp. 3993–3999, May 2011.

[16] J. Gao, M. Kwak, J. Wildeman, A. Herrmann, and M. A. Loi, “Effectiveness of sorting single-walled carbon nanotubes by diameter using polyfluorene derivatives,” *Carbon*, vol. 49, no. 1, pp. 333–338, Jan. 2011.

[17] W. Gomulya, G. D. Costanzo, E. J. F. de Carvalho, S. Z. Bisri, V. Derenskyi, M. Fritsch, N. Fröhlich, S. Allard, P. Gordiichuk, A. Herrmann, S. J. Marrink, M. C. dos Santos, U. Scherf, and M. A. Loi, “Semiconducting Single-Walled Carbon Nanotubes on Demand by Polymer Wrapping,” *Adv. Mater.*, vol. 25, no. 21, pp. 2948–2956, 2013.

[18] H. W. Lee, Y. Yoon, S. Park, J. H. Oh, S. Hong, L. S. Liyanage, H. Wang, S. Morishita, N. Patil, Y. J. Park, J. J. Park, A. Spakowitz, G. Galli, F. Gygi, P. H.-S. Wong, J. B.-H. Tok, J. M. Kim, and Z. Bao, “Selective dispersion of high purity semiconducting single-walled carbon nanotubes with regioregular poly(3-alkylthiophene)s,” *Nat. Commun.*, vol. 2, p. 541, Nov. 2011.

[19] N. Stürzl, F. Hennrich, S. Lebedkin, and M. M. Kappes, “Near Monochiral Single-Walled Carbon Nanotube Dispersions in Organic Solvents,” *J. Phys. Chem. C*, vol. 113, no. 33, pp. 14628–14632, Aug. 2009.

[20] E. S. Snow, P. M. Campbell, M. G. Ancona, and J. P. Novak, “High-mobility carbon-nanotube thin-film transistors on a polymeric substrate,” *Appl. Phys. Lett.*, vol. 86, no. 3, p. 033105, Jan. 2005.
[21] E. S. Snow, J. P. Novak, P. M. Campbell, and D. Park, “Random networks of carbon nanotubes as an electronic material,” *Appl. Phys. Lett.*, vol. 82, no. 13, pp. 2145–2147, Mar. 2003.
[22] Q. Cao, H. Kim, N. Pimparkar, J. P. Kulkarni, C. Wang, M. Shim, K. Roy, M. A. Alam, and J. A. Rogers, “Medium-scale carbon nanotube thin-film integrated circuits on flexible plastic substrates,” *Nature*, vol. 454, no. 7203, pp. 495–500, Jul. 2008.
[23] N. Rouhi, D. Jain, K. Zand, and P. J. Burke, “Fundamental Limits on the Mobility of Nanotube-Based Semiconducting Inks,” *Adv. Mater.*, vol. 23, no. 1, pp. 94–99, 2011.
[24] Y. Miyata, K. Shiozawa, Y. Asada, Y. Ohno, R. Kitaura, T. Mizutani, and H. Shinohara, “Length-sorted semiconducting carbon nanotubes for high-mobility thin film transistors,” *Nano Res.*, vol. 4, no. 10, pp. 963–970, Oct. 2011.
[25] Y. Asada, Y. Miyata, K. Shiozawa, Y. Ohno, R. Kitaura, T. Mizutani, and H. Shinohara, “Thin-Film Transistors with Length-Sorted DNA-Wrapped Single-Wall Carbon Nanotubes,” *J. Phys. Chem. C*, vol. 115, no. 1, pp. 270–273, Jan. 2011.
[26] N. Izard, S. Kazaoui, K. Hata, T. Okazaki, T. Saito, S. Iijima, and N. Minami, “Semiconductor-enriched single wall carbon nanotube networks applied to field effect transistors,” *Appl. Phys. Lett.*, vol. 92, no. 24, p. 243112, Jun. 2008.
[27] P. H. Lau, K. Takei, C. Wang, Y. Ju, J. Kim, Z. Yu, T. Takahashi, G. Cho, and A. Javey, “Fully Printed, High Performance Carbon Nanotube Thin-Film Transistors on Flexible Substrates,” *Nano Lett.*, vol. 13, no. 8, pp. 3864–3869, Aug. 2013.
[28] D. Sun, M. Y. Timmermans, Y. Tian, A. G. Nasibulin, E. I. Kauppinen, S. Kishimoto, T. Mizutani, and Y. Ohno, “Flexible high-performance carbon nanotube integrated circuits,” *Nat. Nanotechnol.*, vol. 6, no. 3, pp. 156–161, Mar. 2011.
[29] S. M. Sze and K. N. Kwok, “Physics of Semiconductor Devices,” no. 3.